JET-ASSISTED DRILLING WITH SUPERCRITICAL CARBON DIOXIDE

J.J. Kollé and M. H. Marvin

ABSTRACT

Under the pressure and temperature conditions found while drilling a typical oil or gas well, carbon dioxide exists as a supercritical fluid; with a density near that of water and extremely low viscosity. These properties should enhance jet erosion of rock and reduce dynamic confinement loads during mechanical drilling in a pressurized borehole. Jet erosion experiments, carried out with CO_2 and water inside a pressurized vessel, show that CO_2 provides much faster cutting of shale and granite and the threshold pressure for jet erosion with CO_2 is significantly lower. The mechanical drilling rate is also much faster when CO_2 is used as a drilling fluid instead of water. Because CO_2-jet-assisted mechanical drilling can provide fast penetration at low bit-weight and torque, it can be used to drill short-radius, lateral drainage wells with low-cost, small-diameter coiled tubing. A model of CO_2 circulation through a coiled tubing drilling system shows that a choke manifold will provide complete control over formation pressures. Cuttings transport in both vertical and horizontal boreholes should be superior to that of water.

INTRODUCTION

Coiled tubing (CT) drilling has become accepted practice for lateral extensions from existing oil and gas wells (Cox et al. 1999). CT has lower thrust and torque capacity than conventional jointed drillstring; furthermore, the torque capacity of small diameter downhole motors is extremely limited. These factors greatly limit the CT drilling rate of penetration. The CT drilling rate of penetration could be increased by providing high pressure fluid jets, however, effective jet erosion drilling requires pressures of at least 100 MPa (14,500 psi) (Maurer 1980, Kollé et al 1991). Although CT is available with yield pressures in excess of 100 MPa; fatigue life considerations, as well as the additional loads on the tubing due to the hanging weight, drilling torque and bending, limit conventional CT operating pressures to well under 100 MPa.

CO_2 is an alternative jet drilling fluid with unique properties that enhance mechanical drilling and jet erosion rates. At the typical pressure and temperature conditions encountered during drilling, CO_2 exists as a supercritical fluid (SC-CO_2) with a density similar to water but the diffusive properties of a gas. Mechanical drilling and high-pressure jet erosion rates should both increase when the drilling fluid can diffuse into the rock (Kollé 1996). The experimental results presented here have verified this prediction.

CO_2-jet-assisted mechanical drilling could be carried out with low-cost, small-diameter CT equipment as shown in Figure 1. Borehole pressure would be controlled with a choke allowing underbalanced drilling; with the capability to quickly transition to overbalance for control of formation pressures. Because CO_2 is non-hydrating and acts as a solvent for heavy hydrocarbons, it will not damage formation permeability and may actually increase conductivity near the wellbore. This approach should prove attractive for drilling short-radius lateral drainage holes to increase oil and gas production.

THERMO-PHYSICAL PROPERTIES OF CARBON DIOXIDE

The phase diagram, triple point and critical point properties for CO_2 are shown in Figure 2. At pressures above the triple point, CO_2 can exist as a liquid. Liquid CO_2 is a relatively incompressible fluid that can be pumped with a positive displacement pump. During drilling operations, the hole bottom pressure is kept high to control formation pressures. At depths greater than 700 m, the hydrostatic pressure is typically greater than the critical pressure of 7.4 MPa. The temperature at this depth is over 31 ºC, because of the earth's geothermal gradient (Press and Siever 1971). Under these conditions, CO_2 is a supercritical fluid with unique properties that should provide superior jet erosion and mechanical rock drilling performance.

Figure 3 shows the equation of state data for CO_2 near the critical point. At 0 °C and pressures greater than 400 MPa (600 psi), liquid CO_2 is relatively incompressible and can be pumped to higher pressure using plunger pumps. In the supercritical state, CO_2 can be used to drive a turbine or positive displacement motor.

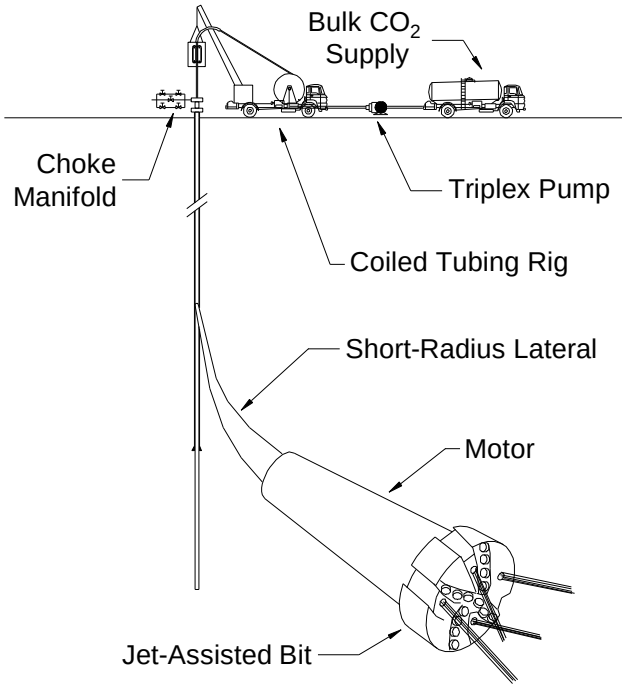

Figure 1. SC-CO_2-jet-assisted CT drilling of short-radius lateral drainage wells.

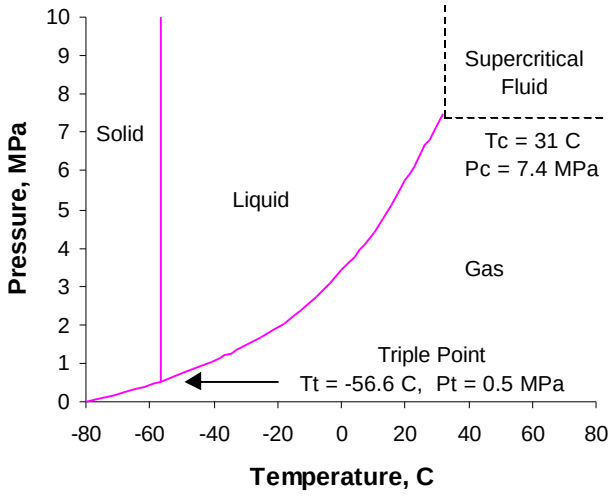

Figure 2. Carbon dioxide phase diagram.

Jet erosion of rock occurs through a mechanism where the fluid jet pressure penetrates behind grains leading to erosion (Crow 1973, Rehbinder 1977). Rock erosion rates are directly proportional the formation permeability and the viscosity and density of the fluid. Figure 4 shows the viscosity of CO_2 under supercritical conditions. The viscosity at the critical point is only .02 cP increasing with pressure to about 0.1 cP at 70 MPa (10,000 psi). The viscosity of SC-CO_2 near the critical point is one to two orders of magnitude smaller than water, while the density remains relatively high. SC-CO_2 should therefore be more effective than water for jet erosion of rock.

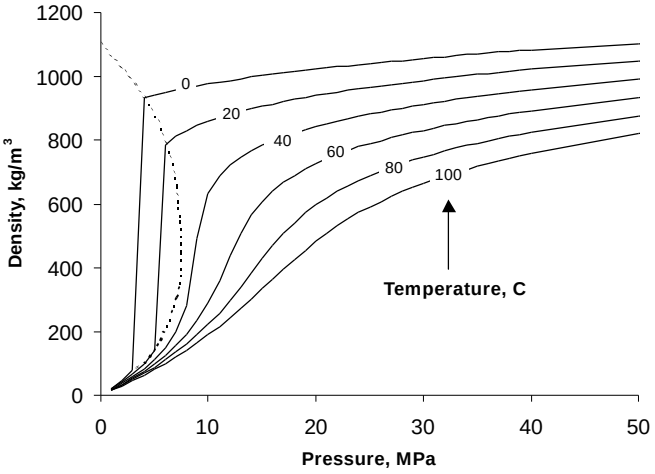

Figure 3. Equation of state data for CO_2 near the critical point (Lemmon et al. 1999).

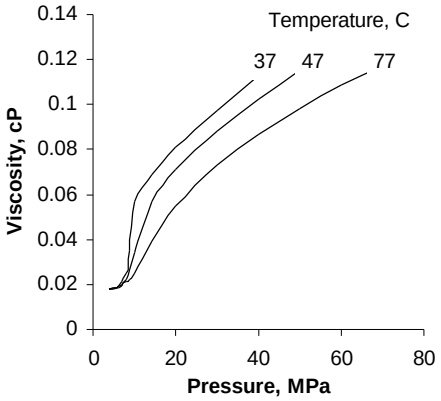

Figure 4. Viscosity of SC-CO_2 (McHugh and Krukonis 1994).

JET EROSION AND PRESSURE DRILLING TESTS

Jet erosion and pressure drilling tests were carried out with water and CO_2 using the flow system shown in Figure 5. CO_2 is supplied from a siphon bottle at a pressure of around 5 MPa. The liquid CO_2 passes through an ice bath at –10 °C before entering an intensifier-type plunger pump. Chilling is necessary to prevent vaporization of the CO_2 as it enters the pump. The fluid supply can be switched from CO_2 to water. Pressure in the test chamber is maintained with a relief valve located downstream of the drill test stand. The test stand was used for high-pressure-jet-erosion tests and mechanical drilling tests.

Jet Erosion Tests

Figure 6 shows the jet erosion test configuration. High pressure fluid (water or CO_2) was pumped through a swivel into a rotating jet head, shown in Figure 7. Cutting tests were carried out on rock samples inside a pressurized vessel held at 13.8 MPa (2000 psi). In each test the jet pressure was increased to a set point while the jet was stationary. The manifold was then rotated for ten seconds at 60 rpm so that the jet made 6 passes over the rock. Figure 8 shows the results of jet kerfing in granite with water and SC-CO_2 at a differential jet pressure of 124 MPa (18,000 psi). The SC-CO_2 jet creates a deeper and wider kerf than the water jet. Figure 9 shows the results of kerfing in Mancos Shale. At a pressure of 193 MPa (28,000 psi) the water jet cut a narrow kerf. The SC-CO_2 jet cut a much deeper, wider kerf at less than half the pressure and only a third the power.

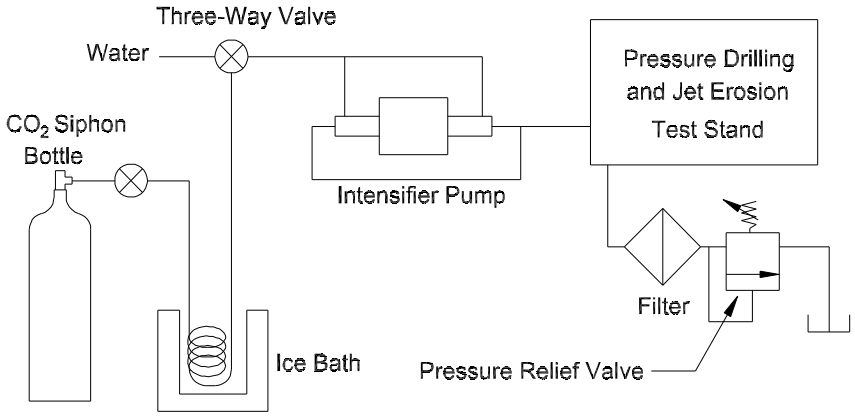

Figure 5. Flow schematic for pressure drilling and jet erosion tests.

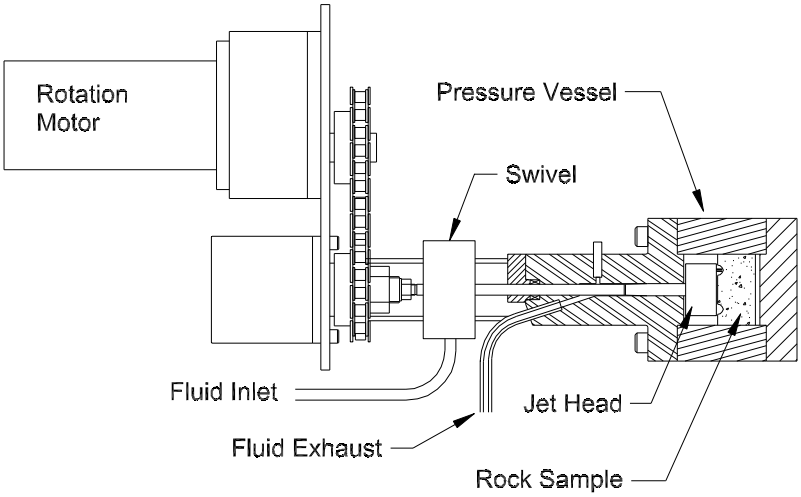

Figure 6. Jet erosion test configuration

Figure 7. Jet head.

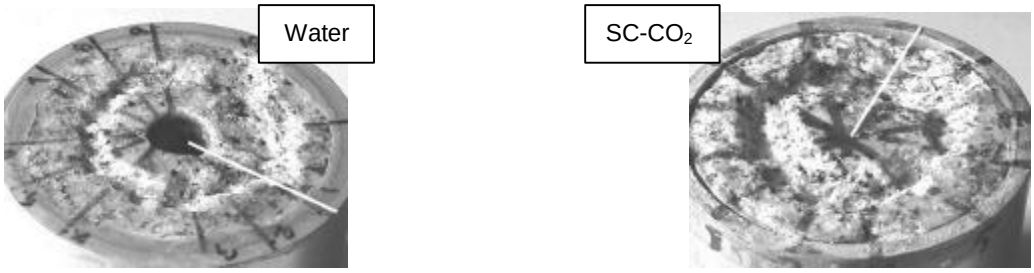

Figure 8. Jet erosion test results in Sierra White Granite, both tests at 124 MPa differential jet pressure. (White lines indicate start of rotation)

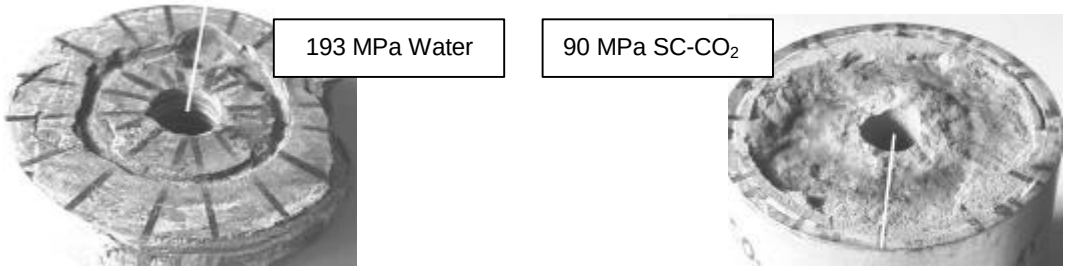

Figure 9. Jet Erosion test results in Mancos Shale (White lines indicate start of rotation).

Jet ErosionThreshold Pressure and Specific Energy

Jet erosion tests were carried out at differential jet pressures increasing from 55 to 193 MPa (8,000 – 28,000 psi). After each test, the rock sample was removed and the cut depth observed at 10 locations. Subsequent cuts were made in the same sample. Figure 10 shows the increasing cut depth as a function of differential jet pressure in both granite and shale.

Cut depths with CO_2 are always greater than with water at the same pressure. The jet erosion threshold pressure is evaluated from this plot by linearly extrapolating the depth curves to zero. The threshold pressures are listed in Table 1. The CO_2 threshold pressure is 2/3rd that of water in the granite and less than half that of water in the shale. Table 1 summarizes the jet erosion data in terms of specific energy of erosion and threshold pressure. The specific energy is defined as the hydraulic power expended divided by the volume of rock removed. It provides a useful means of comparing techniques for drilling and cutting. For jet cutting the relationship is

$$SE_{jet} = \frac{P_{jet} Q_{jet} t_{jet}}{V_{rock}}, \quad (1)$$

where P_{jet} is the differential jet pressure, Q_{jet} is the volumetric flow rate, t_{jet} is the time spent jetting and V_{rock} is the volume of rock removed. The values reported represent the average for all of the cutting tests above the threshold pressure. The specific energy for kerfing granite with SC-CO_2 is less than half that with water and only 3% that of water in Mancos Shale.

Table 1. Jet erosion data summary.

Rock Type	Fluid	SE_{kerf} J/mm^3	P_{th}, MPa
Sierra White Granite	Water	217	75
	CO_2	90	50
	Ratio: CO_2/Water	42%	67%
Mancos Shale	Water	1442	115
	CO_2	38	50
	Ratio: CO_2/Water	3%	44%

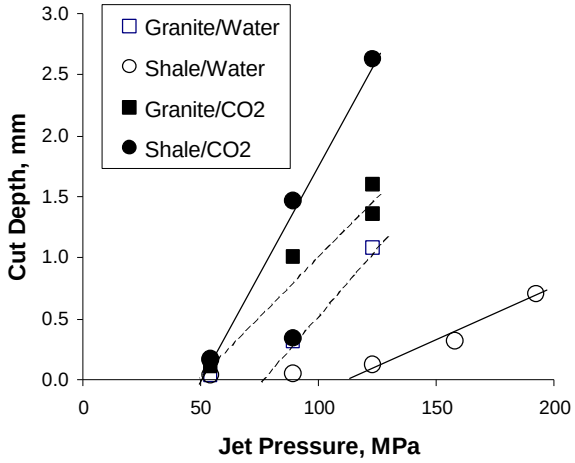

Figure 10. Threshold pressure estimation for shale and granite samples.

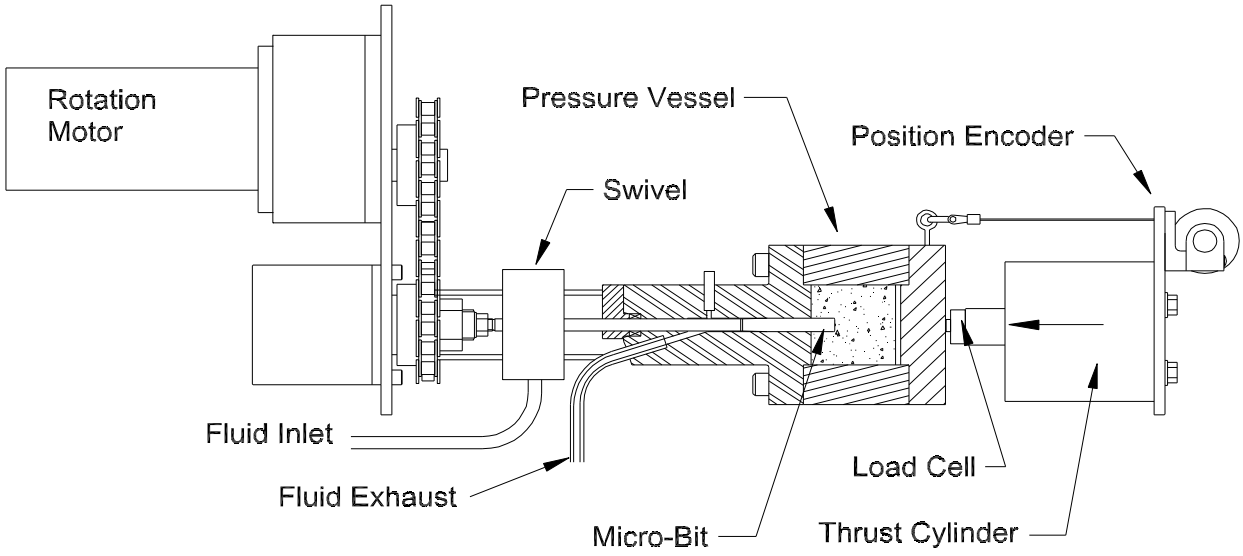

Figure 11. Pressure drilling test configuration.

Figure 12. Microbit with 20 degree backrake carbide cutter.

Table 2. Shale drilling test summary.

Fluid	*ROP*, m/hr	SE_{drill}, J/mm^3
Water	*.23*	1.0
CO_2	*.76*	0.2
Ratio: CO_2/Water	3.3	20%

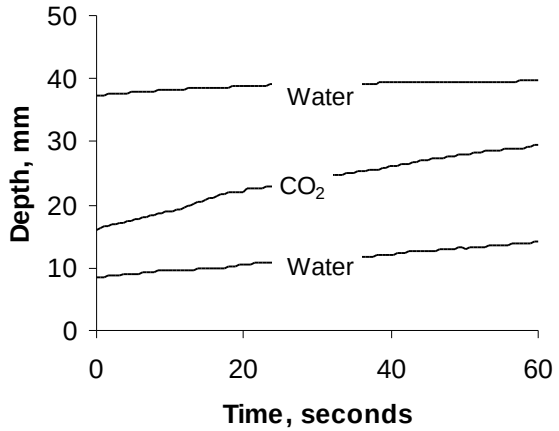

Figure 13. Shale drilling test penetration records.

Pressure Drilling Tests

Mechanical drilling is slowed by borehole pressure and the low viscosity of SC-CO2 compared to water should increase mechanical rock cutting rates. A single small-scale pressure drilling test was carried out in Mancos Shale to evaluate this effect. The drilling test setup is chown in Figure 11. A microbit with a –20 ° backrake cutter (Figure 12) was used for this test. The drilling tests were carried out at a thrust of 200 N and a rotary speed of 60 rpm. The rate of penetration and reaction torque were observed. The depth/time records for the Mancos Shale drilling tests are shown in Figure 11. The sample was first drilled with water. The system was then switched to CO_2 and then back to water.

The mechanical power required for rotary drilling is

$$W_m = \frac{2pNT}{60} \tag{2}$$

where T is the torque on the bit and N is the rotary speed in rpm. The drilling specific energy is the power divided by the hole area times the rate of penetration (*ROP*),

$$SE_{drill} = \frac{W_m}{ROP \cdot A_{hole}}. \tag{3}$$

The shale drilling rate of penetration and specific energy data are summarized in Table 2. The rate of penetration with CO_2 was 3.3 times the rate with water while the drilling specific energy is only about 20% that observed while drilling with water. The reaction torque observed while drilling with CO_2 was slightly smaller than observed drilling with water.

Table 3. CT drilling system operating parameters.

Bulk Storage Pressure	4 MPa	580 psi
Bulk Supply Temperature	-20 °C	
Mass Flow Rate	.5 kg/s	10 gpm
Pump Pressure	70 MPa	10,000 psi
Pump Power	135 kW	181 hp
Coiled Tubing ID	22.9 mm	0.9”
Coiled Tubing OD	31.8 mm	1.25”
Bit/Borehole Diameter	50.8 mm	2”
CT Yield Pressure	137 MPa	19,900 psi
CT Length	2 km	6560’
Pressure Loss in CT	13 MPa	1856 psi
Choke Pressure	5 MPa	725 psi
Bottomhole Pressure	19 MPa	2750 psi
Bottomhole Temperature	70 °C	
Differential Jet Pressure	60 MPa	8700 psi
Jet Power	46 kW	62 hp

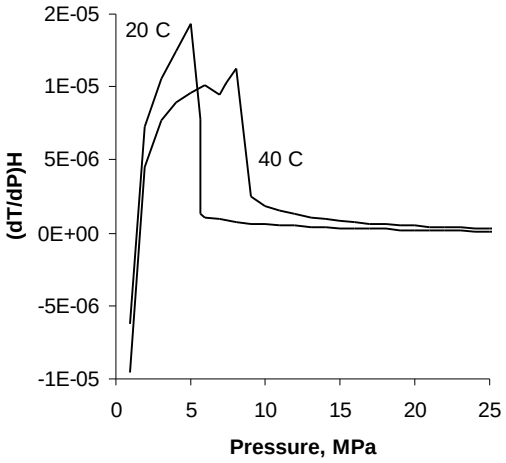

Figure 14. Joule-Thompson coefficients for CO_2.

COILED TUBING DRILLING SYSTEM

As shown above and in other studies (Kollé 1998), mechanical drilling is much more efficient than jet erosion. On the other hand, it is possible to supply much higher hydraulic power than mechanical power through a small-diameter coiled tubing system. Jet-assisted mechanical drilling is the most effective approach. The mechanical cutters break the unsupported ridges of rock that are uncut by the jets. Mechanical cutters also provide better hole gage control than drills that rely on jetting alone. A jet-assisted drilling system using CO_2 would involve high-pressure coiled tubing (CT) operations through surface pressure control equipment as illustrated in Figure 1. Liquid CO_2 from a bulk supply would be pumped through the CT using a high pressure pump. The CO_2 would power a downhole motor that turns a bit with high-pressure jet nozzles and mechanical cutters. Small-diameter vane-motors operating at a pressure of up to 35 MPa (5000 psi) are currently available and higher pressures are possible with heavier housings. Progressive cavity and turbine motors could also be adapted for high pressure CO_2 operation.

Circulation Model

Operating parameters for an example CT drilling system are listed in Table 3. This system is designed to drill a 50.8-mm (2”) diameter hole using a downhole motor. CO_2 is supplied through insulated lines from a refrigerated bulk storage that is insulated and equipped with a refrigeration

unit or a charge of liquid nitrogen to maintain the CO_2 in its fluid state at –20 °C. These tanks are available in sizes of up to 20 tons. A triplex pump boosts the CO_2 pressure to 70 MPa at a rate of 0.5 kg/s (10 gpm liquid CO_2).

A model of CO_2 circulation through a closed loop CT drilling system was implemented to evaluate pressure losses in tubing, borehole pressure and pressures and temperatures in surface equipment. The pressures in the coiled tubing and borehole are determined by first calculating pressure losses with a turbulent Newtonian fluid flow model and integrating the hydrostatic pressure in the overlying fluid. The pressure-density data for SC-CO_2 can be fit by a modified Peng-Robinson equation of state.

$$P = \frac{RT}{(V-b)} - \frac{a}{\left(V^2 + 2Vb - b^2\right)}, \tag{4}$$

where V is the molar volume, R is the gas constant (8.3143 J/mol-°K) and a and b are derived from the critical temperature and pressure;

$$a = \frac{.544R^2T_c^2}{P_c}\left(1 + .76\left(1 - \sqrt{T/T_c}\right)\right)^2$$
$$b = \frac{.0859RT_c}{P_c} \tag{5}$$

The CO_2 flow is modeled using formulas for turbulent Newtonian flow in tubing and the borehole annulus (Monicard, 1982). The turbulent pressure loss for a flow velocity, v, through a length of smooth tubing, L, with diameter, D, is given by

$$\Delta P = \frac{0.1L\,r^{0.8}v^{1.8}m^{0.2}}{D^{1.2}}. \tag{6}$$

The viscosity, m, is assumed to be constant and equal to 5 x 10^{-5} Pa-s, since the pressure loss is relatively insensitive to this parameter. The turbulent pressure loss is sensitive to fluid density, r, which varies significantly in the tubing and borehole annulus.

The model includes effects of Joule-Thompson cooling during expansion through nozzles and chokes. Joule-Thompson cooling coefficients were obtained from entropy in the NIST data tables (Lemmon et al. 1998) and are illustrated in Figure 14. At high pressures, the Joule-Thompson coefficients are low and little cooling takes place. Gas flows through the CT, where it is assumed to come to equilibrium with the borehole temperature (70º C at a depth of 2 km in this example). As indicated in Table 3, the pressure loss in 2-km of CT is only 13 MPa and 45 kW of hydraulic power is available for drilling on the hole bottom. If all the power is used for jet erosion, the rate of penetration would be 2.2 m/hr in Mancos Shale and 0.9 m/hr in Sierra White Granite. Jet assisted mechanical drilling rates should be much higher. Figure 15 shows the circulating density of the CO_2 in the CT and borehole annulus. The annulus density drops at about 350 m as the supercritical fluid becomes a gas. Figure 16 shows the circulating pressure in the borehole annulus. Pressure inside the borehole is controlled with a choke valve manifold located on the surface pressure control stack. At the bottom of the hole, the CO_2 is supercritical. A typical formation pressure curve is shown, with an over-pressurized formation below 1 km. In this example, the borehole would be underbalanced at a depth of 2 km. A lateral hole at a depth of 1 km would be overbalanced.

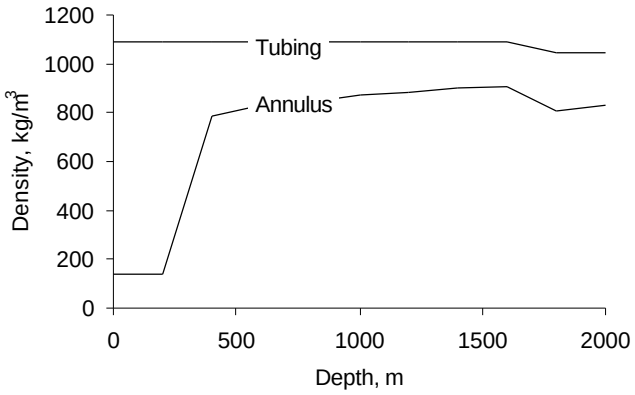

Figure 15. Circulating density of CO_2 in CT and borehole annulus.

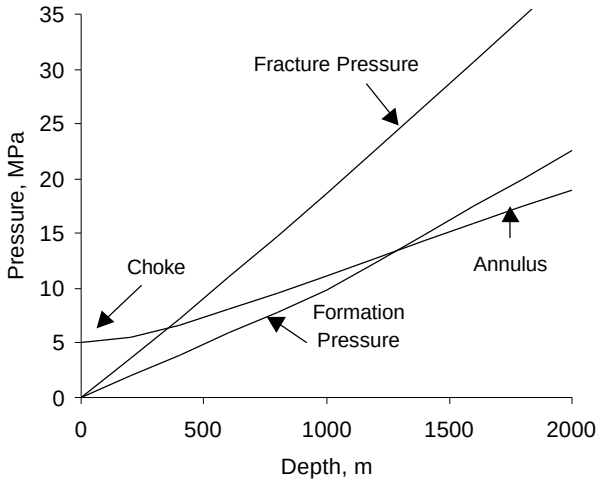

Figure 16. Circulating pressure of CO_2 for example provided in text.

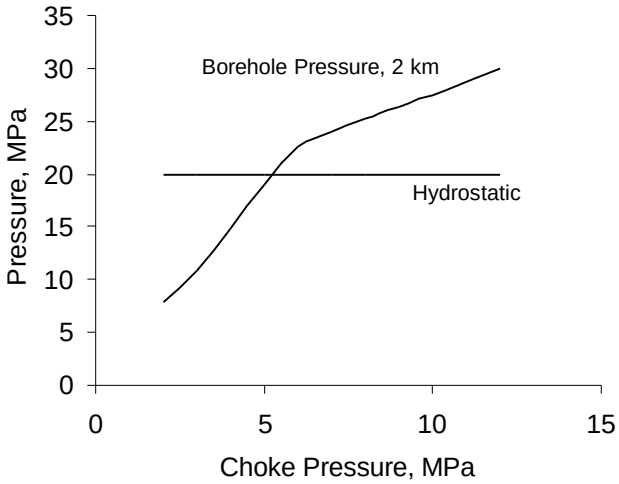

Figure 17. Effect of choke pressure on bottomhole pressure.

The bottomhole pressure can be controlled by adjusting choke pressure as shown in Figure 17. The bottom hole pressure can be quickly adjusted for underbalanced, balanced or overbalanced drilling by controlling the choke. A single fluid system allows for complete well control over a wide range of formation pressure conditions.

The circulation model assumes a Stokes slip velocity model for vertical hole cleaning,

$$v_{slip} = 1.8\sqrt{\frac{g d_p (r_{rock} - r_{gas})}{r_{gas}}}, \qquad (8)$$

where g is the acceleration of gravity (9.8 m/s^2), r_{rock} is the density of rock cuttings and r_{gas} is the gas density. The constant 1.8 represents an empirical fit to the particle slip data provided by Adewumi and Tian (1993) for pneumatic chip transport. As seen in Figure 18, the velocities are sufficient to transport 2-mm diameter particles with a transport ratio (v_{gas}/v_{slip}) greater than 2.

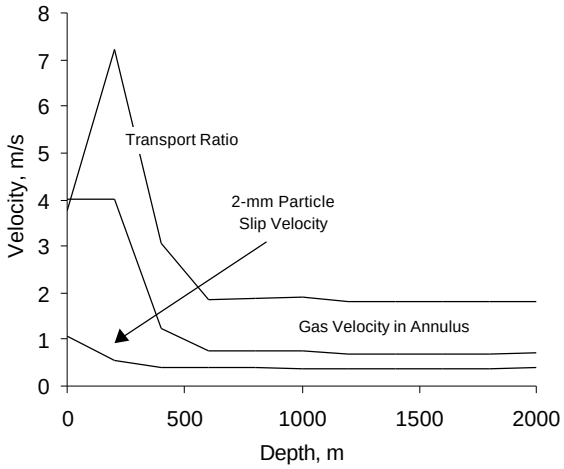

Figure 18. Transport of 2-mm cuttings.

Horizontal hole cleaning typically requires higher velocities than vertical holes in order to ensure turbulent flow. Turbulent flow continuously re-suspends cuttings and prevent buildup of a cuttings bed (Leising and Walton 1998, Adewumi and Tian 1993). The low viscosity and high density of SC-CO_2 in the wellbore annulus will lead to turbulent flow at lower flow velocities than water or drilling mud. The critical flow velocity for turbulence in an annulus is

$$v_c = \frac{2572\mu}{(d_b - d_t)\rho}, \tag{8}$$

where d_b is the hole diameter d_t is the tubing diameter μ is viscosity and ρ is density (Monicard 1982). Note that the critical velocity increases as the annulus size decreases. The critical flow velocity for SC-CO_2 (μ =.0001 Pa-s) in a 51- by 32-mm annulus is .017 m/s (3.3 ft/min). This is $1/10^{th}$ the velocity required for turbulent hole cleaning with water. The annular flow velocity in the example shown in Figure 18 is about 1 m/s, which is much higher than the critical velocity. SC-CO_2 should thus provide excellent hole cleaning in horizontal hole sections.

CONCLUSIONS

Water-jet erosion drilling has not become established practice because of the high threshold pressures and low efficiency of jet erosion in hard rocks such as shale and granite. The unique thermo-physical properties of CO_2 above the supercritical point indicate that it should provide better jet-erosion and mechanical drilling than water-based fluids. Pressure-drilling and jet-erosion tests have confirmed these predictions. SC-CO_2 jet erosion is 40 times more effective than water jet erosion of hard shale and twice as effective as water in granite. The threshold pressure for SC-CO_2 jet-erosion is only 50 MPa in both rock types – less than half the value for water-jet erosion. Pressure drilling tests have shown that CO_2 reduces the drilling specific energy as well.

A circulation model was developed for a CT drilling system designed to operate on CO_2 at 70 MPa. A CO_2-jet-assisted mechanical system operated on a 2-km string of 32-mm CT would provide fast penetration in hard shale and granite. Fluid pressure in the wellbore can be controlled by a surface choke allowing over- or under-balanced drilling. The flow rates and fluid density would provide good hole cleaning in vertical and horizontal wells. The use of small-diameter CT provides a low-cost approach for drilling lateral drainage holes to enhance the production of oil and gas from existing wells.

ACKNOWLEDGMENTS

This work was supported by the U.S. Department of Energy under Contract No. DE-FG03-98ER82696. The intensifier pump system was provided by Flow International Corporation.

REFERENCES

Adewumi, M.A. and S. Tian (1993) "Multiphase hydrodynamic analysis of pneumatic transport of drill cuttings in air drilling," *Powder Technology*, **75**, 133-144.

Cox, R.J., J. Li and G.S. Lupick (1999) "Horizontal underbalanced drilling of gas wells with coiled tubing, *SPE Drilling and Completion*, **14** (1), pp. 3-10.

Crow, S.C. (1973) "A theory of hydraulic rock cutting," *Int. J. Rock Mech. Min.Sci.*, **10**, 567-584.

Kollé, J.J., Otta, R., and Stang, D. L. (1991) "Laboratory and Field Testing of an Ultrahigh-Pressure Jet-Assisted Drilling System," *Proceedings of the 1991 SPE/IADC Drilling Conference*, Paper No. *SPE/IADC 22000*, Amsterdam, pp. 847-56.

Kolle, J.J. (1996) "The effects of pressure and rotary speed on the drag bit drilling strength of deep formations," *SPE 36434*, presented at SPE Annual Technical Conference and Exhibition, 6-9 October 1996, Denver, SPE, Richardson TX.

Kolle, J.J. (1998) "A comparison of water jet, abrasive jet and rotary diamond drilling in hard rock," Proceedings of the 1998 Energy Technology Conference and Exhibition, February 2-4, Houston Texas, ASME New York.

Leising, L.J. and I.C. Walton (1998) Cuttings transport problems and solutions in coiled tubing drilling," *IADC/SPE 39300*, paper presented at IADC/SPE Drilling Conference, Dallas TX 3-6 March 1998.

Lemmon, E.W., M.O. McLinden and D.G. Friend, "Thermophysical Properties of Fluid Systems" *in NIST Chemistry WebBook, NIST Standard Reference Database Number 69*, Eds. W.G. Mallard and P.J. Lindstrom, November 1998, National Institute of Standards and Technology, Gaithersburg MD, 20899 (http://webbook.nist.gov).

Maurer, W.C. (1980) *Advanced Drilling Techniques*, The Petroleum Publishing Company, Tulsa.

Press, F and R. Siever (1974) *Earth*, p. 5

McHugh, M., and V. Kukronis (1994) *Supercritical Fluid Extraction, 2nd ed.* Butterworth-Heinemann, Boston, MA.

Monicard, R. (1982) *Drilling Mud and Cement Slurry Rheology Manual*, Editions Technip, Paris.

Press, F and R. Siever (1974) *Earth*, p. 528, W.H. Freeman and Company, San Francisco.

Rehbinder, G. (1977) "Slot cutting in rock with a high speed water jet," *Int. J. Rock Mech Min. Sci.*, **14**.